JOURNAL OF MATERIALS SCIENCE 17 (1982) 255–262

Transformation toughening

Part 5 *Effect of temperature and alloy on fracture toughness*

F. F. LANGE
Structural Ceramics Group, Rockwell International Science Center, Thousand Oaks, California 91360, USA

The critical stress-intensity factor, K_c, of materials containing tetragonal ZrO_2 was found to decrease with increasing temperature and CeO_2 alloying additions, as predicted by theory. The temperature dependence of K_c was related to the temperature dependence of the chemical free-energy change associated with tetragonal–monoclinic transformation. Good agreement with thermodynamic data available for pure ZrO_2 was obtained when the size of the transformation zone associated with the crack was equated to the size of the ZrO_2 grains. The K_c against CeO_2 addition data was used to estimate the tetragonal, monoclinic, cubic eutectoid temperature of 270° C in the ZrO_2–CeO_2 binary system.

1. Introduction

In Part 2 of this work [1] theory was presented showing that the contribution to fracture toughness, K_c, by a stress-induced transformation is proportional to the chemical free-energy change, $|\Delta G^c|$, associated with the transformation. For the ZrO_2 (tetragonal) $\rightarrow$ ZrO_2 (monoclinic) transformation, $|\Delta G^c|$ is known to decrease with increasing temperature and with alloying ZrO_2 with Y_2O_3, CeO_2 etc. In this part of the series of papers, experiments were designed to measure K_c as a function of temperature and alloy content. The temperature dependence of K_c was measured on polycrystalline ZrO_2 and two-phase Al_2O_3–ZrO_2 materials in which 2 mol% Y_2O_3 was alloyed with the ZrO_2. The fabrication conditions and general properties of these materials have been reported in Part 4 of this work [2].

A series of Al_2O_3–ZrO_2 materials in which CeO_2 was alloyed with the ZrO_2 phase was used to determine the effect of alloy content on K_c. As shown in Fig. 1, CeO_2 was a good candidate for this study since it forms an extensive solid-solution, tetragonal ZrO_2 phase-field and lowers the tetragonal $\rightarrow$ monoclinic transformation temperature to less than 25° C at about 20 mol% CeO_2 addition.* Initial ZrO_2–CeO_2 sintering studies were not successful, i.e., higher CeO_2 contents (added to ZrO_2 powder as a soluble nitrate) resulted in a low-density material. Hot-pressing was avoided, since CeO_2 reduces to Ce_2O_3 in environments produced by graphite dies. Attempts to sinter Al_2O_3–30 vol% ZrO_2 composite powders containing CeO_2 were successful in terms of density and phase content. Thus, these composite materials were chosen for the fracture toughness against alloying content studies.

2. Experimental procedure

2.1. Temperature dependence

Four materials were chosen for this study. Three of these were hot-pressed as detailed in Part 4 [2]: Al_2O_3–29.5 vol% ZrO_2 (plus 2 mol% Y_2O_3), Al_2O_3–45 vol% ZrO_2 (plus 2 mol% Y_2O_3) and ZrO_2 (plus 2 mol% Y_2O_3). The fourth material was an Al_2O_3–30 vol% ZrO_2 (plus 2 mol% Y_2O_3) composite sintered to 97% of theoretical density in air for 1 h at 1600° C in which ZrO_2 was retained in its tetragonal state. The composite powders were prepared for sintering by mixing

*In contrast, the working tetragonal phase-field with Y_2O_3 additions is limited to compositions between 2 and 3 mol% Y_2O_3 in both single-phase tetragonal ZrO_2 [4] and Al_2O_3–ZrO_2 compositions [2].

0022–2461/82/010255–09$02.90/0

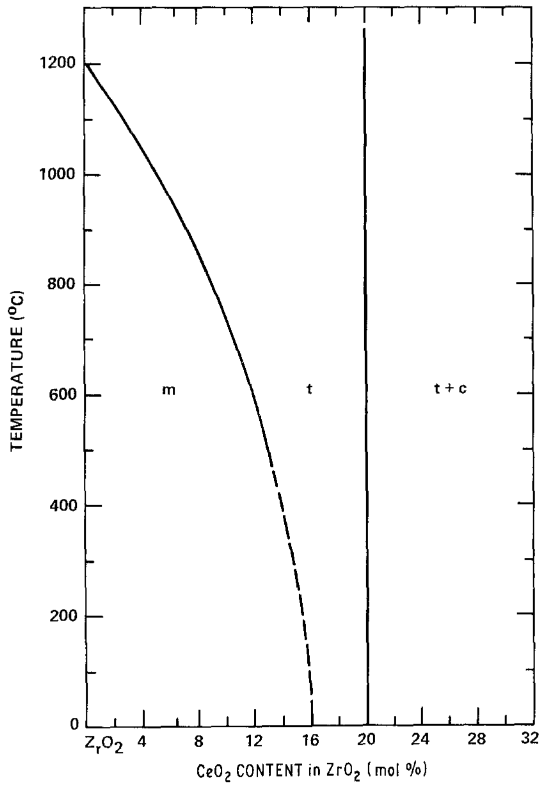

Figure 1 A portion of the ZrO_2–CeO_2 phase diagram [3].

the required weight fractions of Al_2O_3,* ZrO_2† and yttrium nitrate‡ by ball-milling in methanol (Al_2O_3 balls and plastic bottle), drying, calcining at 500° C for 4 h, and isostatic pressing at 350 MPa. Small bar specimens cut from each material were polished in preparation for K_c measurements.

The indentation technique, developed by Evans and Charles [5], was used to measure K_c over the range of − 196° C (liquid nitrogen temperature) to 700° C. A Vickers diamond indentor mounted in tungsten carbide was used with a device which maintained a constant specimen temperature within the range noted. The device consisted of an internally-heated copper post, mounted within a metal flask. The flask was attached to an x–y stage used to translate the specimen relative to the indentor. The stage was mounted on top of a load cell and was insulated from the flask with a machinable ceramic. The specimen was spring-clip loaded in a copper well attached to the post. A chromel–alumel thermocouple, spring-clip loaded to the external face of the specimen, was used to record temperatures. For the K_c measurements at temperatures less than 25° C, the flask was externally insulated and filled with liquid nitrogen. The nitrogen was allowed to slowly evaporate to achieve the desired specimen temperature. For measurements at higher temperatures, the flask was filled with insulating ceramic fibre, and the internal heater was controlled to achieve the desired temperature. Argon was forced into the metal flask to protect the copper parts and diamond from oxidation. Between measurements the indentor was held just above the specimen to avoid a large temperature differential when the indentor was again loaded into the specimen at 20 kg. A single specimen was used for the complete temperature range investigated; two measurements were made at each temperature.

Flexural strength measurements were made with one of the hot-pressed materials [(Al_2O_3–29.5 vol% ZrO_2 (plus 2 mol% Y_2O_3)] over the temperature range in which the K_c measurements were made. Bar specimens (3 mm x 6 mm x > 30 mm) were diamond-cut, ground and then annealed at 1300° C for 24 h to eliminate the surface compressive stresses developed due to the transformation of surface material during grinding [2]. Three strength measurements were made in liquid nitrogen, in a mixture of dry ice and methanol, at room temperature and in air at higher temperatures.

2.3. Effect of alloying

As indicated above, a series of Al_2O_3–30 vol% ZrO_2 composite materials in which CeO_2 was incorporated were found suitable for fracture toughness against alloying content studies. Composite powders containing the appropriate weight fractions of Al_2O_3,§ ZrO_2¶ and CeO_2|| were mixed and milled together in plastic bottles containing methanol and Al_2O_3 mill balls, dried by flash evaporation, calcined at 500° C for 16 h, isostatically pressed into plates and sintered at 1600° C for 1 h. Sixteen compositions containing

*Lindy B, Union Carbide Corp.
†Zircar, Corp.
‡Research Chemicals Corp.
§From Lindy B, Union Carbide Corp.
¶Sub-micrometre ZrO_2, from Zircar Corp.
||Added as Cerrium Nitrate, from Research Chemicals Corp.

CeO_2 contents of between 6 and 22 mol% CeO_2 were fabricated. The densities of these composites ranged between 94% and 98% of theoretical density, based on the density of tetragonal ZrO_2 calculated using the lattice parameters $a = 0.5126$ nm and $c = 0.5224$ nm, as reported by Duwez and Odell [3]. X-ray diffraction analysis of the sintered surfaces showed that 100% of the ZrO_2 was retained in its tetragonal structure for compositions containing $\geqslant 12$ mol% CeO_2. Trace amounts of cubic ZrO_2 were observed for compositions containing 21 and 22 mol% CeO_2, consistent with previous phase equilibria studies [3]. Increasing amounts of monoclinic ZrO_2 were observed as the CeO_2 content decreased from 11 to 6 mol%. Based on these observations, composites containing $\geqslant 11$ mol% CeO_2 were cut and polished for fracture toughness measurements at room temperature, as described above.

3. Results

3.1. Temperature dependence

Fig. 2 illustrates that the fracture toughness decreases with increasing temperature for the four materials investigated. High, low and average values of K_c are defined by the scatter bar at each temperature. These data were fit to a linear equation

$$K_c = A - mT, \qquad (1)$$

where T is temperature in degrees centigrade and the constants A and m are given in Table I.

The flexural strength data for the Al_2O_3–29.3 vol% ZrO_2 (plus 2 mol% Y_2O_3) composites are shown in Fig. 3. These data show that strength decreases with increasing temperature. The dashed line illustrates the expected temperature behaviour of strength, based on the temperature behaviour of K_c, as reported in Table I for this composition and normalizing all data to the room-temperature value.

3.2. Effect of alloying

Fig. 4 reports the K_c data against the CeO_2 addition to the ZrO_2 in the Al_2O_3–30 vol% ZrO_2 sintered materials. Data obtained for the composition containing 11 mol% CeO_2 is low due to its substantial (~ 30%) monoclinic-phase ZrO_2 content. Over the range where only the tetragonal ZrO_2-phase is observed (12 to 20 mol% CeO_2), K_c decreases with increasing CeO_2 content. K_c

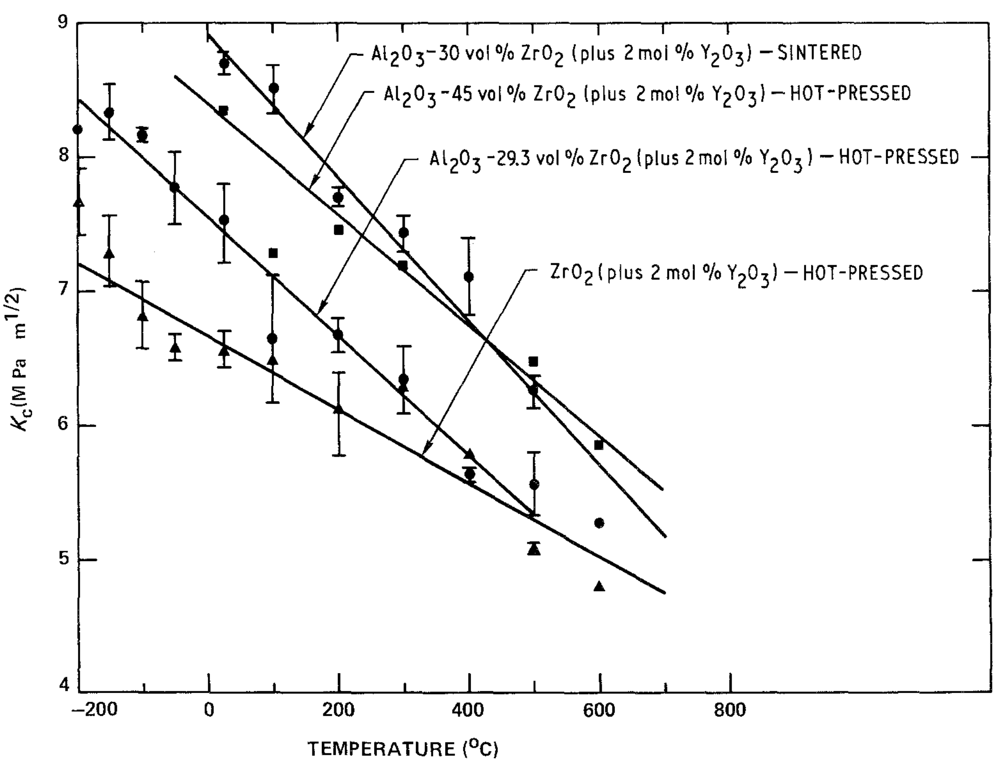

Figure 2 Critical stress-intensity factor plotted against temperature for the four materials investigated.

TABLE I Constants defining the temperature dependence of K_c

Material	Fabriation conditions	A ($MPa\,m^{1/2}$)	m ($MPa\,m^{1/2\circ}\,C^{-1}$)	Correlation coefficient
Al_2O_3–29.3 vol% ZrO_2 (plus 2 mol% Y_2O_3)	Hot-pressed 1600° C/1 h	7.56	0.0044	0.95
Al_2O_3–45 vol% ZrO_2 (plus 2 mol% Y_2O_3)	Hot-pressed 1600° C/1 h	6.78	0.0029	0.92
ZrO_2 (plus 2 mol% Y_2O_3)	Hot-pressed 1600° C/1 h	8.40	0.0041	0.99*
Al_2O_3–30 vol% ZrO_2 (plus 2 mol% Y_2O_3)	Sintered 1600° C/1 h	9.96	0.0054	0.97

*Data at 100° C excluded.

appears to level-off to approximately 6 $MPa\,m^{1/2}$ at the reported tetragonal–cubic phase boundary (compositions containing >20 mol% CeO_2). A linear relation was assumed over the range of 12 to 20 mol% CeO_2, resulting in the relation

$$K_c = 10.32 - 0.202M, \quad (2)$$

where M is the mol% CeO_2 and K_c is in $MPa\,m^{1/2}$.

4. Discussion

In Part 2 [1] of this series of papers, it was shown that the fracture toughness of a brittle material containing a phase which would undergo a stress-induced transformation could be expressed as

$$K_c = \left[K_0^2 + \frac{2V_iE_cR(|\Delta G^c| - \Delta U_{se}f)}{(1-\nu_c^2)}\right]^{1/2}, \quad (3)$$

where K_0 is the critical stress-intensity factor for the composite without the transformation-toughening phenomena, E_c and ν_c are the elastic properties of the material, V_i is the volume fraction of the phase which could undergo the stress-induced transformation, R is the size of the

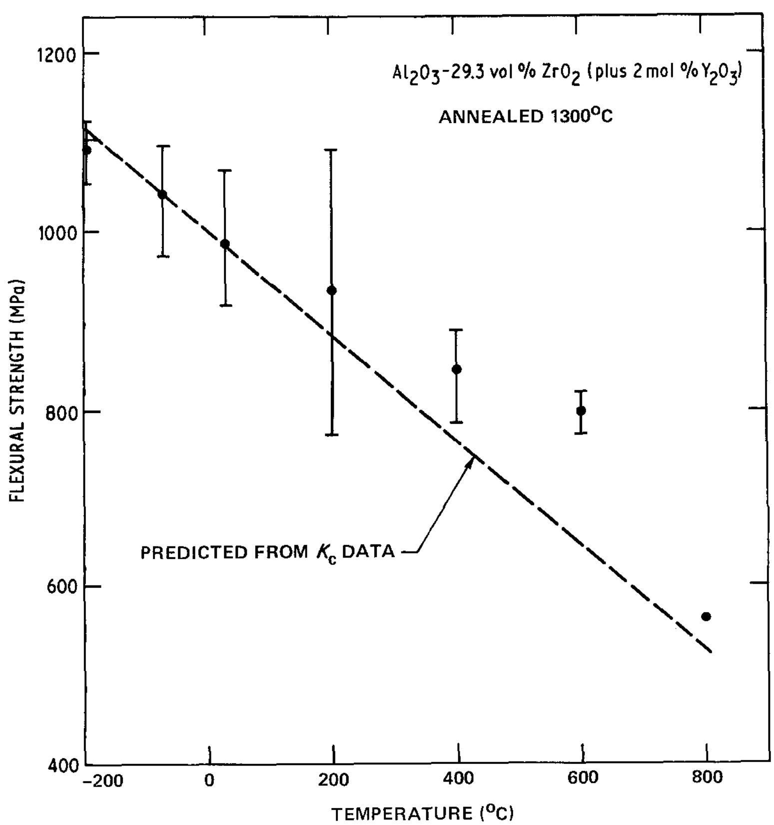

Figure 3 Flexural strength plotted against temperature for the Al_2O_3–29.3 vol% ZrO_2 (plus 2 mol% Y_2O_3) material. Specimens first annealed at 1300° C for 24 h.

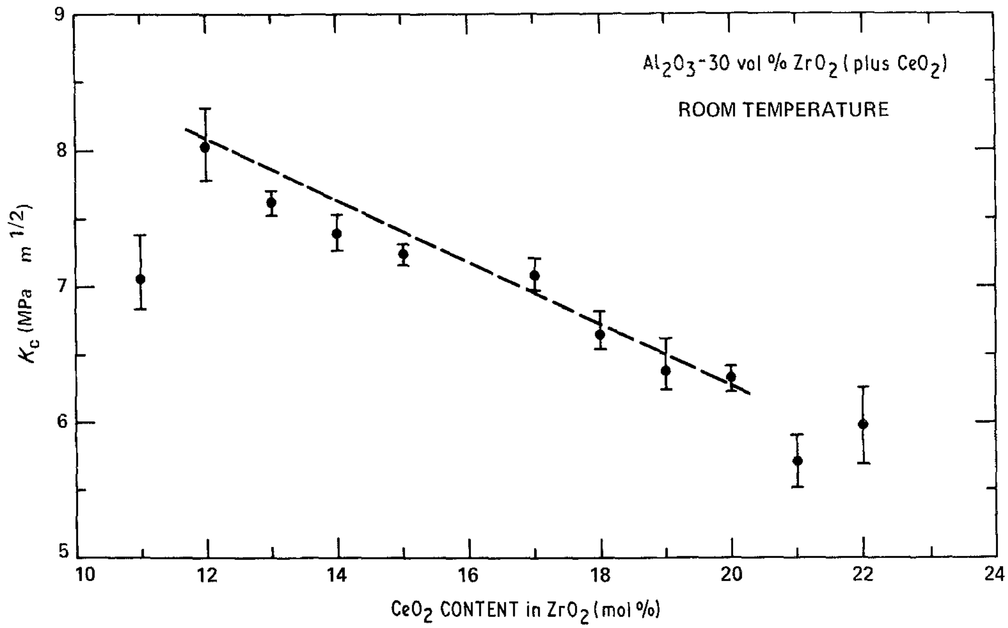

Figure 4 Critical stress-intensity factor plotted against mol% CeO_2 at room temperature.

transformation zone adjacent to the crack and $(|\Delta G^c| - \Delta U_{se} f)$ is the work-loss per unit volume during the stress-induced transformation. Since the magnitude of the chemical free-energy change associated with the transformation, $|\Delta G^c|$, is expected to exhibit the greatest dependence on temperature and alloying, relative to the other factors, it was predicted that the contribution of the stress-induced transformation to fracture toughness (i.e., the second term in Equation 3) would have the same temperature and alloy dependence as $|\Delta G^c|$. Based on the known temperature and alloying dependence of $|\Delta G^c|$ for the $ZrO_2(t) \rightarrow ZrO_2(m)$ transformation, K_c is expected to decrease with increasing temperature and alloying content, which is the general result shown in Figs 2 and 4, respectively. The following paragraphs present a more detailed analysis and discussions of these data with reference to Equation 3.

4.1. Temperature dependence

Based on the assumption that $|\Delta G^c|$ is the only temperature-dependent factor in Equation 3, data obtained during this study and reported in Part 4 [2] of this series of papers were used to calculate $(|\Delta G^c| - \Delta U_{se} f)$ as a function of temperature for comparison with the known temperature dependence of $|\Delta G^c|$ for the transformation of pure ZrO_2 [6]. This calculation started by determining the size of the transformation zone, R, for each material at room temperature, using the average room-temperature value of $(|\Delta G^c| - \Delta U_{se} f)$ calculated in [2] for a series of Al_2O_3–ZrO_2 composites, values of K_0 and E_c reported* for each material in [2] and room-temperature K_c values reported here. Table II lists these values and the resulting value of R, as determined by rearranging Equation 3. It should be noted that in [1], it was hypothesized that $R \simeq$ the grain size; calculated values of R shown in Table II are consistent with the grain sizes of the ZrO_2-phase reported for the hot-pressed materials in [2].

In the next step, values of K_c against temperature, reported in Table I, and the assumed temperature independent values of K_0, E_c, ν_c, V_i and R reported in Table II were used to calculate $(\Delta G^c - \Delta U_{se} f)$ as a function of temperature for each material by rearranging Equation 3. These results are shown in Fig. 5.† Table II also reports the slope of each line $[\delta(|\Delta G^c| - \Delta U_{se} f)/T]$ and the temperature where $(|\Delta G^c| - \Delta U_{se} f) = 0$, (T_0). The fifth line drawn in Fig. 5 is the temperature

*As in [2], ν_c was assumed to be 0.25.

†The four lines coincide at 25° C since it was assumed in Step 1 that all materials had the same value of $(|\Delta G^c| - \Delta U_{se} f)$ at 25° C.

TABLE II Values used to analyse K_c against temperature data

Material	K_c* (MPa m$^{1/2}$)	K_0† (MPa m$^{1/2}$)	$(\Delta G^c - \Delta U_{se}f)$† (MJ m^{-3})	E_c† (GPa)	ν_c†	V_i	R (μm)	$\frac{\delta(\lvert\Delta G^c\rvert - \Delta U_{se}f)}{T}$ (MJm$^{-3\circ}$ C^{-1})	T_0 ($^\circ$C)
Al_2O_3–29.3 vol% ZrO_2 (plus 2 mol% Y_2O_3) (hot-pressed)	7.45	4.10	1.88	333	0.25	0.293	0.99	−0.29	680
Al_2O_3–30 vol% ZrO_2 (plus 2 mol% Y_2O_3) (sintered)	8.83	4.10	188	333	0.25	0.30	1.53	−0.27	730
Al_2O_3–45 vol% ZrO_2 (plus 2 mol% Y_2O_3) (hot-pressed)	8.30	3.70	1.88	285	0.25	0.45	1.10	−0.21	900
ZrO_2 (plus 2 mol% Y_2O_3) (hot-pressed)	6.71	3.90	188	207	0.25	1.00	0.36	−0.24	830
Average of four materials								−0.25	785
ZrO_2 (pure) [6]								−0.25	1200
$Zr_{0.96}Y_{0.04}O_{1.98}$ (ZrO_2 plus 2 mol% 0.5 O_3) [7, 8]									600–830

*Room-temperature values, Table I.
†Room-temperature values, [2].

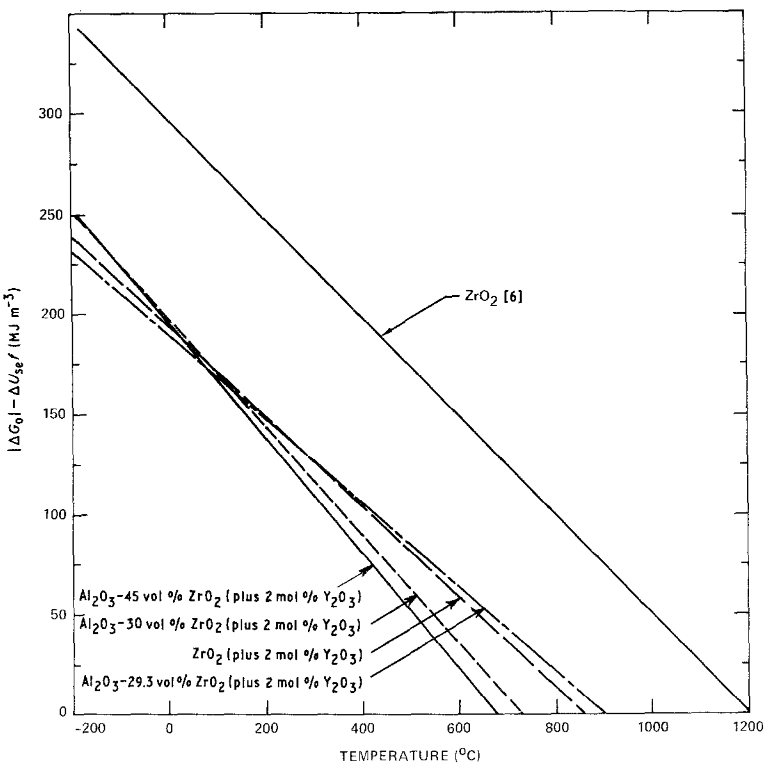

Figure 5 Calculated values of $(|\Delta G^c| - \Delta U_{se}f)$ plotted against temperature for four materials studied. Upper line is $|\Delta G^c|$ against temperature for pure ZrO_2 as determined by Whitney [6].

dependence of $|\Delta G^c|$ for pure ZrO_2, as previously reported by Whitney [6].

The calculations shown in Fig. 5 contain three results, which add greater confidence to the validity of the theoretical fracture mechanics calculations (Equation 3). First, since $|\Delta G^c|$ is expected to exhibit the greatest temperature dependence relative to the other factors in Equation 3, the slopes of the four lines in Fig. 5 should be the same as $\delta|\Delta G^c|/\delta T$ for $Zr_{0.96}Y_{0.04}O_{1.98}$($ZrO_2$ plus 2 mol% Y_2O_3). Although $|\Delta G^c|$ against temperature data do not exist for this solid-solution compound, it is important to note that the slopes are nearly coincident (see Table II) with that of pure ZrO_2, as reported by Whitney [6]. Second, the temperatures T_0, where $(|\Delta G^c| - \Delta U_{se}f) = 0$ lie within the range of transformation temperatures (where $\Delta G^c = 0$), see Table II, for $Zr_{0.96}Y_{0.04}O_{1.98}$ powder [7, 8]. This result suggests that the residual strain energy associated with the ZrO_2 grains that contribute most to the fracture toughness is very small, $\Delta U_{se}f \simeq 0$. Third, the slope of the lines in Fig. 5 critically depend on the chosen value of R, i.e., larger or smaller values of R would not have resulted in the good agreement with $\delta|\Delta G^c|/\delta T$ for pure ZrO_2. Values of R calculated from room-temperature data* (Step 1) not only result in reasonable slopes for $\delta|\Delta G^c|/\delta T$, but they are also in good agreement with the size of the ZrO_2 grains as hypothesized by theory.

4.2. Effect of alloying

Based on the assumption that $|\Delta G^c|$ is the only factor in Equation 3 affected by alloying CeO_2 with ZrO_2, the K_c results presented in Equation 2 have been used to calculate the combined factor $(|\Delta G^c| - \Delta U_{se}f)R$. The linear expression resulting from combining Equations 2 and 3 with the appropriate values [2], $K_0 = 4.1\,\text{MPa}\,\text{m}^{1/2}$, $E_0 = 333\,\text{GPa}$, $\nu_c = 0.25$ and $V_i = 0.30$ for the Al_2O_3–30 vol% ZrO_2 (plus CeO_2) compositions is (in MJ m^{-2})

$$(|\Delta G^c| - \Delta U_{se}f)R \;=\; 415 - 15.8M. \qquad (4)$$

Equation 4 can be used to estimate two thermodynamic properties of ZrO_2, which again

*A second approach can also be used to determine R for each material by calculating the combined product $R(|\Delta G^c| - \Delta U_{se}f)$ in Equation 3 as a function of temperature and assuming that $\delta(|\Delta G^c| - \Delta U_{se}f)/\delta T = 0.248$ MJ m$^{-3°}$ C^{-1} (the value of $\delta|G_c|/\delta T$ for pure ZrO_2) [6]. Using this approach, values of R for the four materials listed in Table II are 1.2, 1.65, 0.95 and 0.34 μm, respectively.

adds greater confidence to the fracture mechanisms theory, as expressed in Equation 3.

First, by extrapolating the data obtained between $M = 12$ to $20\,\text{mol}\%\ CeO_2$ to $M = 0$, one obtains the value of $(|\Delta G^c| - \Delta U_{se}f)R = 415\,\text{MJ}\,\text{m}^{-2}$ for pure ZrO_2. By chosing $R = 1.5\,\mu\text{m}$, the value determined to be consistent with the K_c against temperature data for a similar, sintered Al_2O_3–30 vol% ZrO_2 composite discussed in the last section, one obtains $(|\Delta G^c| - \Delta U_{se}f) = 275\,\text{MJ}\,\text{m}^{-3}$. It is interesting to note that this value agrees almost exactly with the room-temperature value of $|\Delta G^c| = 290\,\text{MJ}\,\text{m}^{-3}$ for pure ZrO_2 as previously calculated by Whitney [6] (see Fig. 5). Although this near-perfect agreement may be fortuitous, it again suggests that the residual strain energy, $\Delta U_{se}f$, associated with the transformed grains adjacent to the crack surfaces can be neglected in estimating their contribution to fracture toughness.

Second, previous phase equilibria work [5] in the ZrO_2–CeO_2 binary system has suggested that CeO_2-additions in the range between 15 and 20 mol% CeO_2 lowers the tetragonal → monoclinic phase transformation temperature below 25° C. K_c measurements (see Fig. 2) clearly show that the tetragonal phase contributes to toughening over the complete range of CeO_2-contents studied (11 to 22 mol%). That is, K_c measurements strongly suggest that the eutectoid temperature is greater than 25° C. Using the fracture-mechanics data, one can estimate the eutectoid temperature by assuming that $\Delta U_{se}f = 0$ and determining the value of M in Equation 4 where $|\Delta G^c|R = 0$. This condition exists when $M = 26$ mol% CeO_2. By constructing a line between 1200° C and 26 mol% CeO_2 on the ZrO_2–CeO_2 phase diagram and recognizing that the tetragonal + cubic phase-field exists when $M = 20$ mol% CeO_2, one estimates the eutectoid temperature to be 270° C, which alters the phase diagram shown in Fig. 1 to that shown in Fig. 6.

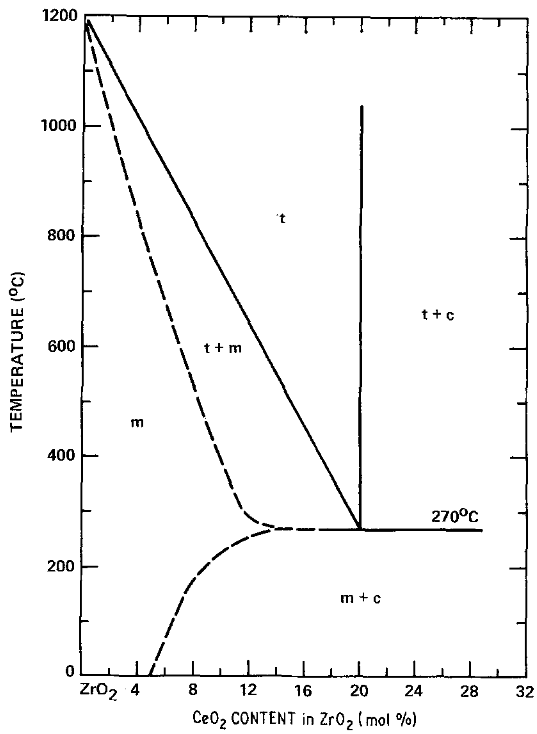

Figure 6 A portion of the ZrO_2–CeO_2 phase diagram, in which the eutectoid temperature has been estimated through fracture-mechanics data.

5. Conclusions

(a) The fracture toughness of materials containing tetragonal ZrO_2 decreased with increasing temperature and alloying addition, consistent with theoretical predictions.

(b) An analysis of the data suggests that the residual strain energy associated with the transformed ZrO_2 grains can be neglected. Thus, the equation which appears to explain the contribution of the stress-induced phase transformation to fracture toughness can be rewritten as

$$K_c = \left[K_0^2 + \frac{2|\Delta G^c|E_c V_i R}{(1-\nu_c^2)}\right]^{1/2}. \qquad (5)$$

(c) The fracture-mechanics data, when analysed with respect to theory as expressed by Equation 3, best fitted the thermodynamic data for ZrO_2 when it was assumed that the size of the transformation zone is the same size as the ZrO_2 grains.

Acknowledgements

The technical assistance of Mr Milan Metcalf was greatly appreciated. This work was supported by the Office of Naval Research under Contract number N00014-77-C-0441.

References

1. F. F. LANGE, *J. Mater. Sci.* **17** (1982) 235.
2. *Idem, ibid.* **17** (1982) 247.
3. P. DUWEZ and F. ODELL, *J. Amer. Ceram. Soc.* **33** (1950) 274.
4. F. F. LANGE, *J. Mater. Sci.* **17** (1982) 240.
5. A. G. EVANS and E. A. CHARLES, *J. Amer. Ceram. Soc.* **59** (1976) 371.

6. E. D. WHITNEY, *J. Amer. Ceram. Soc.* **45** (1962) 612.
7. K. K. SVIRASTOKA, R. N. PATIL, C. B. CHANDRY, K. V. G. K. GOKHALE and E. C. SUBBARO, *Trans. Brit. Ceram. Soc.* 73 (1974) 85.
8. H. G. SCOTT, *J. Mater. Sci.* **10** (1975) 1527.

Received 12 May and accepted 18 June 1981